Aerosol pH and liquid water content determine when particulate matter is sensitive to ammonia and nitrate availability

Athanasios Nenes[1,2*], Spyros N. Pandis[1,3], Rodney J. Weber[4], Armistead Russell[5]

[1]Institute for Chemical Engineering Sciences, Foundation for Research and Technology Hellas, Patras, GR-26504, Greece
[2]School of Architecture, Civil & Environmental Engineering, Ecole polytechnique fédérale de Lausanne, CH-1015, Lausanne, Switzerland
[3]Department of Chemical Engineering, University of Patras, GR-26504, Greece
[4]School of Earth and Atmospheric Sciences, Georgia Institute of Technology, Atlanta, GA 30332, USA
[5]School of Civil & Environmental Engineering, Georgia Institute of Technology, Atlanta, GA 30332, USA

** correspondence to athanasios.nenes@epfl.ch*

Abstract. Nitrogen oxides (NO_x) and ammonia (NH_3) from anthropogenic and biogenic emissions are central contributors to particulate matter (PM) concentrations worldwide. The response of PM to changes in the emissions of both compounds is typically studied on a case-by-case basis, owing in part to the complex thermodynamic interactions of these aerosol precursors with other PM constituents. Here we present a simple but thermodynamically consistent approach that expresses the chemical domains of sensitivity of aerosol particulate matter to NH_3 and HNO_3 availability in terms of aerosol pH and liquid water content. From our analysis, four policy-relevant regimes emerge in terms of sensitivity: *i*) NH_3-sensitive, *ii*) HNO_3-sensitive, *iii*) NH_3 and HNO_3 sensitive, and, *iv*) insensitive to NH_3 and HNO_3. For all regimes, the PM remains sensitive to nonvolatile precursors, such as non-volatile cations and sulfate. When this framework is applied to ambient measurements or predictions of PM and gaseous precursors, the "chemical regime" of PM sensitivity to NH_3 and HNO_3 availability is directly determined. The use of these regimes allows novel insights and is an important tool to evaluate chemical transport models. With this extended understanding, aerosol pH and associated liquid water content naturally emerge as previously ignored state parameters that drive PM formation.

1. Introduction

Gas-phase ammonia ($NH_{3(g)}$, hereon "NH_3") is one of the most important atmospheric alkaline species and contributor to atmospheric fine particle mass (Seinfeld and Pandis, 2016). NH_3 originates from nitrogen-based fertilizer, animal waste (e.g., Aneja et al., 2009), biomass burning (e.g., Behera et al., 2013) and the natural biosphere (NRC, 2016). NH_3 emissions are also linked to world food production, so these are expected to increase with world population (NRC, 2016). Ammonia reacts with sulfuric and nitric acids (from SO_2 and NO_x oxidation) to form ammonium sulfate/bisulfate and nitrate aerosol that globally constitute an important fraction of ambient $PM_{2.5}$ mass (Kanakidou et al., 2005; Sardar et al., 2005; Zhang et al., 2007). SO_2 and NO_x emissions are expected to decrease over time due to air quality regulations (IPCC, 2013). Combined with increasing NH_3 levels (e.g., Skjøth and Geels, 2013), this may lead to changes in aerosol composition and mass concentration, with important impacts on human health (Pope et al., 2004; Lim et al., 2012; Lelieveld et al., 2015; Cohen et al., 2017), ecosystem productivity (Fowler et al., 2013) and the climate system (Haywood and Boucher, 2000; Bellouin et al., 2011; IPCC, 2013).

The above emissions trends have created the expectation that atmospheric aerosol will become significantly less acidic over time (West et al., 1999; Pinder et al., 2007, 2008; Heald et al., 2012; Tsimpidi et al., 2007; Saylor et al., 2015). Reductions in ammonium sulfate due to SO_2 reductions can be balanced, at least in part, by ammonium nitrate formation (e.g., West et al., 1999; Heald et al., 2014; Karydis et al., 2016; Vasilakos et al., 2018). This behavior arises because nitrate may remain in the gas phase as HNO_3 when insufficient amounts of total ammonia (i.e., gas+aerosol) or non-volatile cations (NVCs) from dust and seasalt exist to "neutralize" aerosol sulfate (i.e., completely consume any free sulfuric acid or bisulfate salts). This conceptual model can fail, because it does not sufficiently consider the large volatility difference between deliquesced aerosol containing sulfate/NVCs and ammonium/nitrate the latter two of which is strongly modulated by aerosol acidity (pH) (Guo et al., 2015; Weber et al., 2016; Guo et al., 2017) and changes in the uptake of water due to compositional change. Modeling studies explicitly considering acidity effects may still incorrectly estimate nitrate substitution, owing to errors in emissions of non-volatile cations (such as Na, Ca, K and Mg) that can bias aerosol acidity and ammonium or nitrate partitioning (Vasilakos et al., 2018). A bias in our understanding of aerosol pH can reaffirm a sometimes incorrect conceptual model of aerosol nitrate formation, and fundamental reasons for

prediction biases in nitrate and ammonium (i.e., errors in pH and liquid water content) are not identified – therefore inhibiting further model improvement.

Developing an understanding of when aerosol levels are sensitive to NH_3 and HNO_3 concentrations requires a new approach that explicitly considers aerosol pH and its effects on aerosol precursor volatility in a thermodynamically consistent way. Here we present such a framework, and demonstrate it with observational data to understand the "chemical regimes" associated with aerosol sensitivity to changes in ammonia and nitrate availability.

2. The new conceptual framework

Aerosol pH needs to be sufficiently high for aerosol nitrate formation to readily occur. Depending on the temperature and the amount of liquid water this threshold ranges between a pH of 1.5 and 3.5 (Meskhidze et al., 2003; Guo et al., 2016, 2017; Fig. 1). If pH is high enough, almost all inorganic nitrate forming from NO_x oxidation mostly resides in the aerosol phase; when pH however is low (typically below 1.5 to 2), nitrate remains almost exclusively in the gas phase as HNO_3, regardless of the amount present. Between these "high" and "low" pH values, a "sensitivity window" emerges, where partitioning shifts from nitrate being predominantly gaseous to mostly aerosol-bound. When acidity is below this "pH window", aerosol nitrate is almost nonexistent and therefore aerosol levels are insensitive to HNO_3 availability and controls aimed solely on aerosol nitrate reduction are unimportant since none is in the aerosol phase. When the pH is above the window, most nitrate resides in the aerosol phase, and aerosol levels directly respond to HNO_3 availability. A similar situation exists for aerosol ammonium – although with an inverse dependence on pH, compared to HNO_3. When aerosol pH is low enough any inorganic ammonia emitted mostly resides in the aerosol phase – and when pH is high enough, most of it resides in the gas phase (Fig. 1). Based on the above, one can then define characteristic levels of aerosol acidity, where aerosol becomes insensitive to NH_3 (or HNO_3) concentrations, and vice versa. In the following sections, we quantitatively develop these concepts and formulate a new thermodynamically consistent conceptual framework of aerosol formation.

2.1 Determining when aerosol mass is sensitive to nitric acid and ammonia availability

For a given airmass with total nitrate NO_3^T (i.e., the amount of aerosol and gas-phase nitrate), the equilibrium aerosol nitrate concentration, NO_3^-, is given by $\mathrm{NO_3^-} = \varepsilon(\mathrm{NO_3^-})\ \mathrm{NO_3^T}$, where $\varepsilon(NO_3^-)$ is the fraction of NO_3^T that partitions to the particle phase. Given that when nitrate ion partitions to the aerosol, it is associated with semi-volatile NH_4^+ and nonvolatile cations (NVC) such as Na^+, Ca^{+2}, K^+ and Mg^{+2}, the sensitivity of aerosol mass to changes in NO_3^T is proportional to the changes occurring in $\mathrm{NO_3^-}$. Therefore:

$$\frac{\partial PM}{\partial \mathrm{NO_3^T}} = \zeta \frac{\partial \mathrm{NO_3^-}}{\partial \mathrm{NO_3^T}} = \zeta \varepsilon(\mathrm{NO_3^-}) \quad (1)$$

where ζ is the ratio of PM mass formed (or lost) per mol of NO_3^- that condenses (or evaporates) from the particles. Therefore, if NO_3^- is associated with aerosol NH_4NO_3, then ζ = 80/62=1.29. Lower values are found for particles rich in NVC that are associated with carbonates and chlorides; for example, if nitric acid were replacing chloride in seasalt (e.g., conversion of NaCl to $NaNO_3$), the ratio would be ζ = (85-58.4)/62=0.43. A similar ζ is seen when alkaline dust particles rich in $CaCO_3$ react with HNO_3 to form $Ca(NO_3)_2$, ζ=(164-100)/(2×62)=0.51. Given that NVCs tend to reside in the coarse mode aerosol, environments that are rich in NH_3 and form large amounts of NH_4NO_3 (e.g., in the North Europe, Midwest of the US, China) would therefore tend to exhibit ζ~1.29; in environments where there is a mixture of NVC and NH_4NO_3, then ζ would be a weighted average between 1.29 (pure NH_4NO_3 limit) and 0.5 (NVC limit), determined by the ratio of the two cation categories in the aerosol. The sensitivity of PM to changes in NO_3^T can therefore be expressed in terms of nitrate partitioning, so the parameters that affect $\varepsilon(\mathrm{NO_3^-})$ also directly impacts $\frac{\partial PM}{\partial \mathrm{NO_3^T}}$.

We now proceed with explicitly quantifying how aerosol liquid water and pH affect nitrate partitioning, hence PM sensitivity to nitrate availability. Meskhidze et al. (2003) and later on Guo et al. (2017) showed that for a deliquesced aerosol $\varepsilon(NO_3^-)$ explicitly depends on the concentration of H^+ in the aerosol phase, $[\mathrm{H^+}]$, and the aerosol liquid water content, W_i, as:

$$\varepsilon(\mathrm{NO_3^-}) = \frac{K_{n1} H_{HNO_3} W_i RT}{\gamma_{H^+}\gamma_{NO_3^-}[\mathrm{H^+}] + K_{n1} H_{HNO_3} W_i RT} \quad (2)$$

where H_{HNO_3}, K_{n1} is the Henry's law and acid dissociation constant for HNO_3, respectively, R is the universal gas constant, T is the temperature and $\gamma_{H^+}, \gamma_{NO_3^-}$ are the single-ion activity coefficients for H^+, NO_3^-, respectively. Temperature dependence for H_{HNO_3} is provided by Sander (2015), while activity coefficients can be calculated using an aerosol thermodynamic model (e.g., ISORROPIA-II; Fountoukis et al., 2007).

Similarly, equilibrium partitioning of NH_3^T to the aerosol is given by $NH_4^+ = \varepsilon(NH_4^+)\ NH_3^T$, where $\varepsilon(NH_4^+)$ is the fraction of NH_3^T (i.e., the amount of aerosol ammonium and gas-phase ammonia) that partitions to the particle phase. The sensitivity of aerosol mass to perturbations in total ammonia is $\frac{\partial PM}{\partial NH_3^T} = \lambda \frac{\partial NH_4^+}{\partial NH_3^T} = \lambda \varepsilon(NH_4^+)$, where λ is the ratio of mass of PM that is lost/gained per mol of evaporation/loss of NH_4^+. λ is more variable than ζ, because the anion associated with ammonium can be involatile or semi-volatile species with relatively large molar mass. For example, if NH_4^+ condenses/evaporates from sulfate salts (NH_4HSO_4, $(NH_4)_2SO_4$), then λ = 18/17 = 1.06, λ = 4.4 for NH_4NO_3, λ = 2.97 for NH_4Cl and λ=10 for $(NH_4)_2(COO)_2$. Given that the majority of the aerosol ammonium is associated with nitrate and sulfates, aerosol therefore tends to exhibit λ that is a weighted average of ~ 1 (NH_4HSO_4, $(NH_4)_2SO_4$ limit) and 4.4 (NH_4NO_3 limit), determined by the aerosol SO_4/NO_3 ratio. In regions where the aerosol is acidic, nitrate tends to reside in the gas phase and λ ~ 1.

From the above, the sensitivity of PM to changes in NH_3^T can be expressed in terms of its partitioning. $\varepsilon(NH_4^+)$, as in Eq. 2, can be linked to aerosol liquid water and pH (Guo et al., 2017):

$$\varepsilon(NH_4^+) = \frac{\frac{\gamma_{H^+}}{\gamma_{NH_4^+}} \frac{H_{NH_3}}{K_a} [H^+] W_i RT}{1 + \frac{\gamma_{H^+}}{\gamma_{NH_4^+}} \frac{H_{NH_3}}{K_a} [H^+] W_i RT} \quad (3)$$

where H_{NH_3}, K_a is the Henry's law and dissociation constant for NH_3, respectively, and $\gamma_{NH_4^+}$ is the single-ion activity coefficient for NH_4^+, respectively. Temperature dependence for H_{NH_3} is provided by Sander (2015).

Defining the parameters $\Psi = \frac{RTK_{n1}H_{HNO_3}}{\gamma_{H^+}\gamma_{NO_3^-}}$ and $\Phi = \frac{\gamma_{H^+}}{\gamma_{NH_4^+}} \frac{H_{NH_3}}{K_a} RT$, equations (2) and (3) can be written as:

$$\varepsilon(\mathrm{NO_3^-}) = \frac{\Psi W_i}{[\mathrm{H^+}] + \Psi W_i};\ \varepsilon(\mathrm{NH_4^+}) = \frac{\Phi[\mathrm{H^+}]W_i}{1 + \Phi[\mathrm{H^+}]W_i} \quad (4)$$

For given levels of W_i, Equations (4) yield "sigmoidal" functions that display a characteristic "pH sensitivity window", where the partition fraction changes from zero to unity over a limited pH range. Equations (4) can then be used to determine a "characteristic pH" that defines when aerosol is insensitive to total ammonia and nitrate availability (or emissions). For this purpose, we determine the pH for which $\varepsilon(\mathrm{NO_3^-})$ and $\varepsilon(\mathrm{NH_4^+})$ are equal to a characteristic (small) threshold value, being α for $\varepsilon(\mathrm{NO_3^-})$ and β for $\varepsilon(\mathrm{NH_4^+})$ (Figure 1). When α (or β) are exceeded, the aerosol is said to be sensitive to NH_3 (or NO_x) emissions, because changes in NH_3, NO_x levels can appreciably affect aerosol concentrations. This sensitivity may be in one direction (e.g., increase of the emissions if the corresponding particulate levels are low and decrease if they are high) or in both. Guo et al. (2018) found a "critical" pH of approximately 3, above which the $\varepsilon(\mathrm{NO_3^-})$ is nearly 1 and almost all nitrate ($\mathrm{NO_3^T}$) resides in the aerosol phase. Here we generalize the approach developing relationships between the terms that depend on aerosol composition, pH and particle water, with temperature still remaining as an independent variable.

Based on the above discussion, the characteristic acidity level for nitrate, *pH'*, is computed as

$$\alpha = \frac{\Psi W_i}{[H^+]' + \Psi W_i} \Longrightarrow [H^+]' = \frac{(1-\alpha)}{\alpha}\Psi W_i \Longrightarrow$$
$$pH' = -log\left[\left(\frac{1-\alpha}{\alpha}\right)\Psi W_i\right] \quad (5)$$

where $[H^+]'$ is the concentration where $\varepsilon(\mathrm{NO_3^-})$ equals the threshold value. The parameter $\left(\frac{1-\alpha}{\alpha}\right)$, which we call the "threshold factor", adjusts pH' to account for the threshold above which the aerosol is said to become sensitive to $\mathrm{NO_3^T}$.

Similarly to nitrates, the characteristic acidity level for ammonium, $pH^{"}$, is determined as

$$\beta = \frac{\Phi[\mathrm{H^+}]W_i}{1 + \Phi[\mathrm{H^+}]W_i} \Longrightarrow [\mathrm{H^+}] = \frac{1}{\frac{(1-\beta)}{\beta}\Phi W_i} \Longrightarrow$$
$$pH^{"} = log\left[\left(\frac{1-\beta}{\beta}\right)\Phi W_i\right] \quad (6)$$

2.2 Chemical domains of aerosol mass sensitive to nitrate and ammonia perturbations

Hereon we consider $\alpha = \beta = 0.1$; in selecting these threshold values, we assume that aerosol responds in an important manner to NH_3/HNO_3 emissions when at least 10% of the total precursor can partition to the aerosol phase. The threshold can be adjusted accordingly to fit any other objective, depending on the analysis required (e.g., a prescribed PM response). With these considerations, the threshold factors are 9 for both compounds and the characteristic pH values obtain the very simple formulations $pH' = -log[9\Psi W_i]$ for nitrate and $pH^{"} = log[9\Phi W_i]$ for ammonium. Apart from the value of the parameters Ψ, Φ (which vary mainly with T), pH' and pH" vary only with W_i – with a logarithmic dependence. Figure 2 displays their variation for 273 K (panel a) and 298 K (panel b). Nitrate tends to exhibit a decrease in pH' with increasing W_i, and vice-versa for ammonium and $pH^{"}$.

Based on the values of the characteristic pH and its relation to the aerosol pH, we can then determine whether the aerosol responds to changes in nitrate or ammonium – as only when pH > pH' (or pH < pH") does the aerosol become sensitive to changes in NO_3^T (or NH_3^T). This realization constitutes the basis of our new framework and aerosol can belong to one of four distinct chemical regimes:

- Regime 1: Not sensitive to either NH_3 or HNO_3: this occurs when pH > pH" and pH < pH'. This regime is termed "*NH_3, HNO_3 insensitive*" or just "*Insensitive*".
- Regime 2: Not sensitive to NH_3; sensitive to HNO_3: this occurs when pH > pH" and pH > pH'. This regime is termed "*HNO_3 sensitive*".
- Regime 3: *Sensitive to both* NH_3 *and* HNO_3: this occurs when pH < pH" and pH < pH' pH > pH'. This regime is termed "*NH_3, HNO_3 sensitive*".
- Regime 4: *Sensitive to* NH_3 *and not sensitive to* HNO_3: pH< pH" and pH < pH' pH > pH'. This regime is termed "*NH_3 sensitive*".

Figure 3 indicates these four regions in white (Regime 1), blue (Regime 2), purple (Regime 3), and red (Regime 4) for 273 K (Figure 3a) and 298 K (Figure 3b). Therefore, any specific set of data (from observations or a model), based on its corresponding aerosol acidity and liquid water, places it on one of the 4 above domains - which in turn determines the "chemical regime" of aerosol response to NH_3^T and/or NO_3^T. What is surprising is the emergence of a region of conditions where aerosol is insensitive to either NH_3 or HNO_3 – which occupies an increasingly large pH-LWC domain as the temperature increases (Fig.3).

A characteristic point on the chemical regime map corresponds to where the two lines "crossover", thus separating Regime 1 from Regime 3, and Regime 2 from Regime 4. This "critical" point corresponds to a characteristic value of LWC, W_i^*, that is easily found by equating pH' with pH":

$$W_i^* = \left[\left(\frac{1-\alpha}{\alpha}\right)\left(\frac{1-\beta}{\beta}\right)\Phi\Psi\right]^{-1/2} \quad (7)$$

Substitution of W_i^* into either Eq. 5 or 6 gives also the characteristic pH^* of this crossover point:

$$pH^* = -\frac{1}{2}log\left(\frac{\Psi}{\Phi}\right) \quad (8)$$

Both pH^*, W_i^* depend on temperature (Fig. 3). For T=298K and $\alpha = \beta = 0.1$, $\Psi \sim 7.38\times10^2$, $\Phi \sim 1.67\times10^7$ so $W_i^* \sim 3.5$ μg m^{-3} and $pH^* \sim 2.2$. Therefore, for moderately acidic aerosol (pH*~2) and for moderate levels of liquid water content (a few μg m^{-3} liquid water content) aerosol tends to be insensitive to emissions of either NH_3^T and NO_3^T precursors. For higher (or lower) pH levels, the aerosol transitions between regions 2 (or 4). For liquid water above W_i^*, there is a "transition pH" from an ammonia-sensitive to an exclusively nitrate-sensitive aerosol, which depends linearly on liquid water content (Fig. 3). Similarly, there is also another "transition pH" that defines when the aerosol becomes exclusively sensitive to NH_3^T.

As formulated here, the framework does not imply that the water is associated with the species considered (ammonium, nitrate) but rather it is treated as a variable; pH is also treated as a variable and can be modulated from organics, NVCs, halogen ions, sulfates, carbonates, and other species. The main requirement is that the aerosol is dominated by a single aqueous phase, as discussed in Battaglia et al. (2019) and references therein – therefore the framework applies more accurately to conditions where the relative humidity is above 40% and the assumption of thermodynamic equilibrium is applicable (i.e., ultra-viscosity and semi-solid effects do not considerably limit mass transfer in the aerosol phase). Given the complexity of aerosol thermodynamics, it is remarkable that such an apparently simple framework can be used to characterize the regions of aerosol sensitivity to NH_3^T and NO_3^T emissions, with "coordinates" being pH and liquid water. This is illustrated in the following section.

3. Application of framework

The above framework requires knowledge of aerosol pH and liquid water content, which can be routinely calculated by state-of-the-art atmospheric chemical transport models (e.g., CMAQ, CAMx) during the course of any simulation. Thermodynamic analysis of ambient aerosol and gas-phase data also provides aerosol pH and liquid water content, therefore the above framework can be used to characterize the chemical domain of ambient and simulated aerosol.

The applicability of the chemical domain approach is demonstrated by its application to ambient data. For this purpose, we have selected more than 7700 data points obtained from observations over 5 locations worldwide: Cabauw (CBW), Tianjin (TJN), California (CNX), SE US (SAS), and a wintertime NE USA (WIN) study (Table 1). Each dataset displays a broad range of acidity, temperature, relative humidity and has been thoroughly studied and evaluated for the applicability of thermodynamic analysis. Each data point corresponds roughly to a 1-hr measurement, meaning that the chemical domains examined correspond to effectively the instantaneous response of PM to ammonia and nitric acid availability. In addition to the major aerosol species ammonium/ammonia, sulfate, nitrate/nitric acid, the datasets also contain chloride/hydrochloric acid, sodium, calcium, potassium and magnesium (not shown in Table 1) which contribute to the pH and liquid water levels predicted. However, not all of the data provide size-dependent composition, so our analysis is limited, here, to looking at the bulk fine PM composition. The range of $\varepsilon(\mathrm{NO_3^-})$ and $\varepsilon(\mathrm{NH_4^+})$ for all the data examined is presented in Figure 4. Noted on the figure are also indicative domains that correspond to Regions 1 to 4. It is clear that each dataset has distinct characteristics that provide insight on the expected sensitivity of PM to NH_3 and HNO_3 emissions – as low $\varepsilon(\mathrm{NO_3^-})$, $\varepsilon(\mathrm{NH_4^+})$ correspond to low sensitivity of PM to their respective precursor emissions. It is unclear however, based on ε alone, where this (in)sensitivity originates from; strong/weak acidity, high/low liquid water content or high/low temperature. The latter is important, given that those parameters in models shape the local sensitivity profiles. Much of the data are found towards the extremes in the partitioning fraction scale, leaving the central part of the diagram sparsely populated. However, this does not mean that aerosols are limited by one component or the other, as much of the data are found to be in the region sensitive to both.

Figure 5 presented the chemical domain classifications for each location. These data sets are used to provide an example and may not apply to all locations in the region. For each subplot, the characteristic curves are calculated using the average temperature of the dataset (presented in Table

1). From each subplot it becomes clear that every location (CBW, TJN, CNX, SAS, WIN) belongs almost exclusively to a characteristic domain for the duration of the measurements. Cabauw, for example, is characterized by high enough NH_3 so that aerosol is not sensitive to variations of it. Nitric acid, on the other hand, is by far a limiting factor in PM formation, hence CBW is in the HNO_3-dominated regime throughout the year. For similar reasons, Tianjin is also mostly in the HNO_3-dominated region, although a fraction of the data points lie in the combined NH_3-HNO_3 region owing to the slightly more acidic conditions compared to CBW. The Southeast US (SAS) is considerably more acidic, and with an order of magnitude less liquid water content compared to CBW and TJN; for these reasons it belongs to the NH_3-sensitive regime (i.e., there is little NH_4NO_3 present in summer – even if total nitrate availability may be high). The California dataset is quite interesting, being one that partly occupies the insensitive region and then transitions to the combined NH_3-HNO_3 region; in this dataset, the combination of moderate NH_3 levels, temperature and the fraction of NVCs from sea-salt that is internally mixed with the other components make aerosol sensitive to both NH_3 and HNO_3 variations. The wintertime eastern US dataset (WIN) corresponds to a broad region (aircraft data set), hence the data naturally occupies multiple domains. The lower temperatures, however, prohibit most of the data from occupying any of the insensitive region; most of the data occupies the NH_3-sensitive regime, owing to the strong acidity and low liquid water. One remarkable point, however, is that regardless of location, the transition point between NH_3-dominated and HNO_3-dominated sensitivity always occurs at a pH around 2 but at variable levels of liquid water content. The latter is important, as pH emerges as a required but not sufficient condition to determine the type of aerosol sensitivity; too little water (i.e., liquid water below the characteristic value W_i^*) and the aerosol can be insensitive to NH_3, even if the pH is as low as 2 (Figure 5a). In the case of Cabauw conditions (Figure 5a), where aerosol liquid water ranges from 7-15 μg m^{-3}, the "transition pH" from an aerosol that is exclusively sensitive to NO_3^T precursor emissions to one that is sensitive to both NH_3^T and NO_3^T ranges from 2.8 and 3.2, which is in perfect agreement with the analysis of Guo et al. (2018). The additional insight that our framework shows is that the "transition pH" varies with temperature and logarithmically with aerosol liquid water content, in response to emissions and diurnal/seasonal variability and climate change. This insight, not apparent in the analysis of Guo et al. (2018), demonstrates the power and flexibility of the new framework.

4. Conclusions

Here we present a simple yet powerful way to understand when concentrations of nitric acid (HNO_3) and ammonia (NH_3) from anthropogenic and biogenic emissions can considerably modulate particulate matter (PM) concentrations worldwide. The conceptual framework explicitly considers acidity (pH), aerosol liquid water content and temperature as the main parameters controlling secondary inorganic PM sensitivity and identifies four policy-relevant regimes: *i*) NH_3-dominated, *ii*) HNO_3-dominated, *iii*) both NH_3 and HNO_3, and, *iv*) a previously unidentified domain where neither NH_3 nor HNO_3 are important for PM formation (but only nonvolatile precursors such as NVCs and sulfate). When this framework is applied to ambient measurements and predictions of PM and gaseous precursors, the "chemical regime" of PM sensitivity to emissions is directly determined, allowing novel insights and eventually an important tool to evaluate models, given that if simulated aerosol is in the same sensitivity regime as suggested by thermodynamic analysis of observations – models are expected to provide plausible responses to changes in aerosol emissions. The framework can be used to identify regions or time periods where pH and liquid water content prediction errors matter for PM sensitivity assessments. With this deeper understanding, aerosol pH and associated liquid water content naturally emerge as policy-relevant parameters that have not been explicitly explored until now.

Competing interests

The authors declare that they have no conflicts of interest.

Acknowledgements

This work was supported by the project PyroTRACH (ERC-2016-COG) funded from H2020-EU.1.1. - Excellent Science - European Research Council (ERC), project ID 726165. We also acknowledge support from the U.S. EPA under grant R83588001. Its contents are solely the responsibility of the grantee and do not necessarily represent the official views of the supporting agencies. Further, the U.S. government does not endorse the purchase of any commercial products or services mentioned in the publication. We also thank Hongyu Guo and Guoliang Shi for providing access to the data used here.

Code and Data availability

User access to data used in this manuscript is described in the citations referenced for each dataset, and can also be accessed from the compiled dataset of Pye et al. (2019). The ISORROPIA-II thermodynamic equilibrium code is available at http://isorropia.epfl.ch.

Author contributions

AN initiated the study, developed the framework, carried out analysis of the data and wrote the initial draft. All authors provided feedback on the analysis approach and extensively commented on the manuscript.

References

Aneja, V. P., Schlesinger, W. H., and Erisman, J. W.: Effects of Agriculture upon the Air Quality and Climate: Research, Policy, and Regulations, Environ. Sci. Technol., 43, 4234-4240, doi: 10.1021/es8024403, 2009.

Battaglia, M. A. Jr., Weber, R.J., Nenes, A., Hennigan, C.J. (2019) Effects of Water-soluble Organic Carbon on Aerosol pH, *Atmos.Chem.Phys.*, in press.

Behera, S. N., Sharma, M., Aneja, V. P., and Balasubramanian, R.: Ammonia in the atmosphere: a review on emission sources, atmospheric chemistry and deposition on terrestrial bodies, Environ. Sci. Pollut. Res. Int., 20, 8092-8131, doi: 10.1007/s11356-013-2051-9, 2013.

Bellouin, N., Rae, J., Jones, A., Johnson, C., Haywood, J., and Boucher, O.: Aerosol forcing in the Climate Model Intercomparison Project (CMIP5) simulations by HadGEM2-ES and the role of ammonium nitrate, J. Geophys. Res., 116, D20206, doi: 10.1029/2011jd016074, 2011.

Cohen, A. J., Brauer, M., Burnett, R., Anderson, H. R., Frostad, J., Estep, K., Balakrishnan, K., Brunekreef, B., Dandona, L., Dandona, R., Feigin, V., Freedman, G., Hubbell, B., Jobling, A., Kan, H., Knibbs, L., Liu, Y., Martin, R., Morawska, L., Pope, C. A., Shin, H., Straif, K., Shaddick, G., Thomas, M., van Dingenen, R., van Donkelaar, A., Vos, T., Murray, C. J. L., and Forouzanfar, M. H.: Estimates and 25-year trends of the global burden of disease attributable to ambient air

pollution: an analysis of data from the Global Burden of Diseases Study 2015, Lancet, 389, 1907-1918, doi: 10.1016/s0140-6736(17)30505-6, 2017.

Fountoukis, C., and Nenes, A.: ISORROPIA II: a computationally efficient thermodynamic equilibrium model for K^+-Ca^{2+}-Mg^{2+}-NH_4^+-Na^+-SO_4^{2-}-NO_3^--Cl^--H_2O aerosols, Atmos. Chem. Phys., 7, 4639-4659, doi: 10.5194/acp-7-4639-2007, 2007.

Fowler, D., Coyle, M., Skiba, U., Sutton, M. A., Cape, J. N., Reis, S., Sheppard, L. J., Jenkins, A., Grizzetti, B., Galloway, J. N., Vitousek, P., Leach, A., Bouwman, A. F., Butterbach-Bahl, K., Dentener, F., Stevenson, D., Amann, M., and Voss, M.: The global nitrogen cycle in the twenty-first century, Philos. Trans. R. Soc. B, 368, 20130164, doi: 10.1098/rstb.2013.0164, 2013.

Guo, H., Xu, L., Bougiatioti, A., Cerully, K. M., Capps, S. L., Hite, J. R., Carlton, A. G., Lee, S. H., Bergin, M. H., Ng, N. L., Nenes, A., and Weber, R. J.: Fine-particle water and pH in the southeastern United States, Atmos. Chem. Phys., 15, 5211-5228, doi: 10.5194/acp-15-5211-2015, 2015.

Guo, H., Sullivan, A. P., Campuzano-Jost, P., Schroder, J. C., Lopez-Hilfiker, F. D., Dibb, J. E., Jimenez, J. L., Thornton, J. A., Brown, S. S., Nenes, A., and Weber, R. J.: Fine particle pH and the partitioning of nitric acid during winter in the northeastern United States, J. Geophys. Res., 121, 10355-10376, doi: 10.1002/2016jd025311, 2016.

Guo, H., Liu, J., Froyd, K. D., Roberts, J. M., Veres, P. R., Hayes, P. L., Jimenez, J. L., Nenes, A., and Weber, R. J.: Fine particle pH and gas–particle phase partitioning of inorganic species in Pasadena, California, during the 2010 CalNex campaign, Atmos. Chem. Phys., 17, 5703-5719, doi: 10.5194/acp-17-5703-2017, 2017.

Guo, H., R. Otjes, P. Schlag, A. Kiendler-Scharr, A. Nenes, and R. J. Weber: Effectiveness of ammonia reduction on control of fine particle nitrate, Atm. Chem. Phys., 18, 12241-12256, 2018.

Haywood, J., and Boucher, O.: Estimates of the direct and indirect radiative forcing due to tropospheric aerosols: A review, Rev. Geophys., 38, 513-543, doi: 10.1029/1999rg000078, 2000.

Heald, C. L., Collett Jr., J. L., Lee, T., Benedict, K. B., Schwandner, F. M., Li, Y., Clarisse, L., Hurtmans, D. R., Van Damme, M., Clerbaux, C., Coheur, P.-F., Philip, S., Martin, R. V., and Pye, H. O. T.: Atmospheric ammonia and particulate inorganic nitrogen over the United States, Atmos. Chem. Phys., 12, 10295–10312, https://doi.org/10.5194/acp-12-10295-2012, 2012.

IPCC: Climate Change 2013: The Physical Science Basis. Contribution of Working Group I to the Fifth Assessment Report of the Intergovernmental Panel on Climate Change., Cambridge, United Kingdom and New York, NY, USA, 1535, 2013.

Kanakidou, M., Seinfeld, J. H., Pandis, S. N., Barnes, I., Dentener, F. J., Facchini, M. C., Van Dingenen, R., Ervens, B., Nenes, A., Nielsen, C. J., Swietlicki, E., Putaud, J. P., Balkanski, Y., Fuzzi, S., Horth, J., Moortgat, G. K., Winterhalter, R., Myhre, C. E. L., Tsigaridis, K., Vignati, E., Stephanou, E. G., and Wilson, J.: Organic aerosol and global climate modelling: a review, Atmos. Chem. Phys., 5, 1053-1123, doi: 10.5194/acp-5-1053-2005, 2005.

Karydis, V. A., Tsimpidi, A. P., Pozzer, A., Astitha, M., and Lelieveld, J.: Effects of mineral dust on global atmospheric nitrate concentrations, Atmos. Chem. Phys., 16, 1491–1509, https://doi.org/10.5194/acp-16-1491-2016, 2016.

Lelieveld, J., Evans, J. S., Fnais, M., Giannadaki, D., and Pozzer, A.: The contribution of outdoor air pollution sources to premature mortality on a global scale, Nature, 525, 367-371, doi: 10.1038/nature15371, 2015.

Lim, S. S., Vos, T., Flaxman, A. D., Danaei, G., Shibuya, K., Adair-Rohani, H., AlMazroa, M. A., Amann, M., Anderson, H. R., Andrews, K. G., Aryee, M., Atkinson, C., Bacchus, L. J., Bahalim, A. N., Balakrishnan, K., Balmes, J., Barker-Collo, S., Baxter, A., Bell, M. L., Blore, J. D., Blyth, F., Bonner, C., Borges, G., Bourne, R., Boussinesq, M., Brauer, M., Brooks, P., Bruce, N. G., Brunekreef, B., Bryan-Hancock, C., Bucello, C., Buchbinder, R., Bull, F., Burnett, R. T., Byers, T. E., Calabria, B., Carapetis, J., Carnahan, E., Chafe, Z., Charlson, F., Chen, H., Chen, J. S., Cheng, A. T.-A., Child, J. C., Cohen, A., Colson, K. E., Cowie, B. C., Darby, S., Darling, S., Davis, A., Degenhardt, L., Dentener, F., Des Jarlais, D. C., Devries, K., Dherani, M., Ding, E. L., Dorsey, E. R., Driscoll, T., Edmond, K., Ali, S. E., Engell, R. E., Erwin, P. J., Fahimi, S., Falder, G., Farzadfar, F., Ferrari, A., Finucane, M. M., Flaxman, S., Fowkes, F. G. R., Freedman, G., Freeman, M. K., Gakidou, E., Ghosh, S., Giovannucci, E., Gmel, G., Graham, K., Grainger, R., Grant, B., Gunnell, D., Gutierrez, H. R., Hall, W., Hoek, H. W., Hogan, A., Hosgood Iii, H. D., Hoy, D., Hu, H., Hubbell, B. J., Hutchings, S. J., Ibeanusi, S. E., Jacklyn, G. L., Jasrasaria, R., Jonas, J. B., Kan, H., Kanis, J. A., Kassebaum, N., Kawakami, N., Khang, Y.-H., Khatibzadeh, S., Khoo, J.-P., Kok, C., Laden, F., Lalloo, R., Lan, Q., Lathlean, T., Leasher, J. L., Leigh, J., Li, Y., Lin, J. K., Lipshultz, S. E., London, S., Lozano, R., Lu, Y., Mak, J., Malekzadeh, R., Mallinger, L., Marcenes, W.,

March, L., Marks, R., Martin, R., McGale, P., McGrath, J., Mehta, S., Memish, Z. A., Mensah, G. A., Merriman, T. R., Micha, R., Michaud, C., Mishra, V., Hanafiah, K. M., Mokdad, A. A., Morawska, L., Mozaffarian, D., Murphy, T., Naghavi, M., Neal, B., Nelson, P. K., Nolla, J. M., Norman, R., Olives, C., Omer, S. B., Orchard, J., Osborne, R., Ostro, B., Page, A., Pandey, K. D., Parry, C. D. H., Passmore, E., Patra, J., Pearce, N., Pelizzari, P. M., Petzold, M., Phillips, M. R., Pope, D., Pope Iii, C. A., Powles, J., Rao, M., Razavi, H., Rehfuess, E. A., Rehm, J. T., Ritz, B., Rivara, F. P., Roberts, T., Robinson, C., Rodriguez-Portales, J. A., Romieu, I., Room, R., Rosenfeld, L. C., Roy, A., Rushton, L., Salomon, J. A., Sampson, U., Sanchez-Riera, L., Sanman, E., Sapkota, A., Seedat, S., Shi, P., Shield, K., Shivakoti, R., Singh, G. M., Sleet, D. A., Smith, E., Smith, K. R., Stapelberg, N. J. C., Steenland, K., Stöckl, H., Stovner, L. J., Straif, K., Straney, L., Thurston, G. D., Tran, J. H., Van Dingenen, R., van Donkelaar, A., Veerman, J. L., Vijayakumar, L., Weintraub, R., Weissman, M. M., White, R. A., Whiteford, H., Wiersma, S. T., Wilkinson, J. D., Williams, H. C., Williams, W., Wilson, N., Woolf, A. D., Yip, P., Zielinski, J. M., Lopez, A. D., Murray, C. J. L., and Ezzati, M.: A comparative risk assessment of burden of disease and injury attributable to 67 risk factors and risk factor clusters in 21 regions, 1990–2010: a systematic analysis for the Global Burden of Disease Study 2010, Lancet, 380, 2224-2260, doi: 10.1016/S0140-6736(12)61766-8, 2012.

Meskhidze, N., Chameides, W. L., Nenes, A., and Chen, G.: Iron mobilization in mineral dust: Can anthropogenic SO_2 emissions affect ocean productivity?, Geophys. Res. Lett., 30, 2085, doi: 10.1029/2003gl018035, 2003.

National Academies of Sciences, Engineering, and Medicine: The Future of Atmospheric Chemistry Research: Remembering Yesterday, Understanding Today, Anticipating Tomorrow Washington, DC: The National Academies Press. DOI: 10.17226/235730, 2016.

Pinder, R. W., Adams, P. J., and Pandis, S. N.: Ammonia Emission Controls as a Cost-Effective Strategy for Reducing Atmospheric Particulate Matter in the Eastern United States, Environ. Sci. Technol., 41, 380-386, doi: 10.1021/es060379a, 2007.

Pinder, R. W., Dennis, R. L., and Bhave, P. V.: Observable indicators of the sensitivity of PM2.5 nitrate to emission reductions—Part I: Derivation of the adjusted gas ratio and applicability at regulatory-relevant time scales, Atmos. Environ., 42, 1275-1286, doi: 10.1016/j.atmosenv.2007.10.039, 2008a.

Pope, C. A., III, Burnett, R. T., Thurston, G. D., Thun, M. J., Calle, E. E., Krewski, D., and Godleski, J. J.: Cardiovascular mortality and long-term exposure to particulate air pollution: epidemiological evidence of general pathophysiological pathways of disease, Circulation, 109, 71-77, doi: 10.1161/01.CIR.0000108927.80044.7F, 2004.

Pye, H. O. T., Nenes, A., Alexander, B., Ault, A. P., Barth, M. C., Clegg, S. L., Collett Jr., J. L., Fahey, K. M., Hennigan, C. J., Herrmann, H., Kanakidou, M., Kelly, J. T., Ku, I.-T., McNeill, V. F., Riemer, N., Schaefer, T., Shi, G., Tilgner, A., Walker, J. T., Wang, T., Weber, R., Xing, J., Zaveri, R. A., and Zuend, A.: The Acidity of Atmospheric Particles and Clouds, Atmos. Chem. Phys. Discuss., https://doi.org/10.5194/acp-2019-889, in review, 2019

Seinfeld, J.H. and Pandis, S.N.: Atmospheric Chemistry and Physics: From Air Pollution to Climate Change. John Wiley & Sons, Hoboken, 2016.

Sander, R.: Compilation of Henry's law constants (version 4.0) for water as solvent, Atmos. Chem. Phys., 15, 4399-4981, 2015.

Sardar, S. B., Fine, P. M., and Sioutas, C.: Seasonal and spatial variability of the size-resolved chemical composition of particulate matter (PM10) in the Los Angeles Basin, J. Geophys. Res., 110, D07S08, doi: 10.1029/2004jd004627, 2005.

Saylor, R., Myles, L., Sibble, D., Caldwell, J., and Xing, J.: Recent trends in gas-phase ammonia and $PM_{2:5}$ ammonium in the southeast United States, J. Air Waste Manage., 65, 347–357,

https://doi.org/10.1080/10962247.2014.992554, 2015.

Shi, X., Nenes, A., Xiao, Z., Song, S., Yu, H., Shi, G., Zhao, Q., Chen, K., Feng, Y., Russell, A.G.: High-resolution datasets unravel the effects of sources and meteorological conditions on nitrate and its gas-particle partitioning, Env.Sci.Tech., 53 (6), pp 3048–3057, 2019.

Skjøth, C. A., and Geels, C.: The effect of climate and climate change on ammonia emissions in Europe, Atmos. Chem. Phys., 13, 117-128, doi: 10.5194/acp-13-117-2013, 2013.

Tsimpidi, A. P., Karydis, V. A., and Pandis, S. N.: Response of inorganic fine particulate matter to emission changes of sulfur dioxide and ammonia: The Eastern United States as a case study, J Air Waste Manan. Assoc., 57, 1489-1498, doi: 10.3155/1047-3289.57.12.1489, 2007.

Vasilakos, P., Russell, A., Weber, R., and Nenes, A.: Understanding nitrate formation in a world with less sulfate, Atmos. Chem. Phys. Disc., 1-27, doi: 10.5194/acp-2018-406, 2018.

Weber, R. J., Guo, H., Russell, A. G., and Nenes, A.: High aerosol acidity despite declining atmospheric sulfate concentrations over the past 15 years, Nat. Geosci., 9, 282-285, doi: 10.1038/ngeo2665, 2016.

West, J. J., Ansari, A. S., and Pandis, S. N.: Marginal $PM_{2.5}$: nonlinear aerosol mass response to sulfate reductions in the eastern United States, J. Air Waste Manage., 49, 1415–1424, 1999.

Zhang, Q., Jimenez, J. L., Canagaratna, M. R., Allan, J. D., Coe, H., Ulbrich, I., Alfarra, M. R., Takami, A., Middlebrook, A. M., Sun, Y. L., Dzepina, K., Dunlea, E., Docherty, K., DeCarlo, P. F., Salcedo, D., Onasch, T., Jayne, J. T., Miyoshi, T., Shimono, A., Hatakeyama, S., Takegawa, N., Kondo, Y., Schneider, J., Drewnick, F., Borrmann, S., Weimer, S., Demerjian, K., Williams, P., Bower, K., Bahreini, R., Cottrell, L., Griffin, R. J., Rautiainen, J., Sun, J. Y., Zhang, Y. M., and Worsnop, D. R.: Ubiquity and dominance of oxygenated species in organic aerosols in anthropogenically-influenced Northern Hemisphere midlatitudes, Geophys. Res. Lett., 34, L13801, doi: 10.1029/2007gl029979, 2007.

Table 1. Characteristics of the datasets used for determining the sensitivity to NH_3 and HNO_3 emissions. Shown is the average relative humidity (RH), Temperature (K), and the concentration of major aerosol precursors (μg m^{-3}), while in the respective standard deviation for each parameter is shown in parenthesis. Access to the data is described in the *Data Availability* section.

Dataset ID, Location, (Reference)	***RH* (%)**	***Temp. (K)***	***Sulfate* (μg μ^{-3})**	***Total Ammonium* (μg μ^{-3})**	***Total Nitrate* (μg μ^{-3})**
TJN, Tianjin, China (Shi et al., 2019; Pye et al. 2019)	56.6 (12.4)	301.8 (2.79)	21.46 (10.99)	37.74 (7.68)	18.12 (11.50)
CNX, Pasadena, CA, USA (Guo et al., 2017; Pye et al. 2019)	71.3 (15.5)	291.1 (4.26)	2.86 (1.70)	3.44 (1.81)	10.23 (9.74)
CBW, Cabauw, Netherlands (Guo et al., 2018; Pye et al. 2019)	78.2 (14.8)	282.2 (7.3)	1.92 (1.57)	9.3 (6.8)	4.1 (3.9)
WIN, Eastern USA (Guo et al., 2016; Pye et al. 2019)	56.1 (18.9)	270.8 (6.52)	1.02 (0.08)	0.53 (0.44)	2.12 (2.08)
SAS, Centerville, AL, USA (Guo et. al, 2015; Pye et al. 2019)	72.7 (17.4)	297.9 (3.45)	1.81 (1.18)	0.78 (0.50)	0.12 (0.15)

Figure Captions

Figure 1. Particle phase fraction of total nitrate, $\varepsilon(NO_3^-)$ (blue curve) and total ammonium, $\varepsilon(NH_4^+)$ (red curve) versus pH for a temperature of 288 K and an aerosol liquid water content of (a) 10 μg m^{-3}, and, (b) 0.5 μg m^{-3}. The blue-color zone denotes where aerosol responds strongly (i.e. $\frac{\partial NO_3^-}{\partial NO_3^T} \sim 1$) to the amount of total nitrate, orange where NH_3 dominates (i.e. $\frac{\partial NH_4^+}{\partial NH_3^T} \sim 1$), purple where both NH_3 and HNO_3 changes affect PM concentrations, and white where aerosol is relatively insensitive to NH_3 and HNO_3 fluctuations. In defining the sensitivity domains, we have assumed that a partitioning fraction of 10% (black dotted lines), and its corresponding "characteristic" pH, defines where the aerosol becomes insensitive to changes in total NH_3, HNO_3.

Figure 2. Characteristic pH for defining when aerosol is sensitive to changes in available nitrate (blue lines) and ammonia (red lines) versus W_i. Results shown for a temperature of 298 K (dashed line) and 273 K (solid line). Note the relatively stronger effects of temperature changes on the characteristic pH for nitrate. Calculations carried out using the Excel sheet provided in the supplement.

Figure 3. Chemical domains of aerosol response to ammonia and nitrate emissions. Shown are results for 273 K (panel a) and 298 K (panel b). Note that there exists a fairly expansive region of acidity and liquid water content (especially for warmer temperatures) where aerosol is relatively insensitive to ammonia and nitrate emissions; here only non-volatiles (sulfate, NVCs) can have an appreciable impact on aerosol mass. Also important is the role of aerosol water in helping define the chemical regime of aerosol sensitivity to precursors.

Figure 4. Aerosol partitioning fraction for total ammonia/ammonium and nitric acid/nitrate for the 5 regions examined: a) Cabauw - CBW, b) CalNex - CNX, c) Tianjin – TJN, d) SOAS – SAS, and, e) E. United States (WIN).

Figure 5. Chemical domains of sensitivity of aerosol to NH_3 and NO_x emissions for 5 regions examined: a) Cabauw - CBW, b) CalNex - CNX, c) Tianjin – TJN, d) SOAS – SAS, and, e) E. United States (WIN). Average composition, temperature and humidity along with their variations (expressed by their standard deviation) is provided in Table 1.

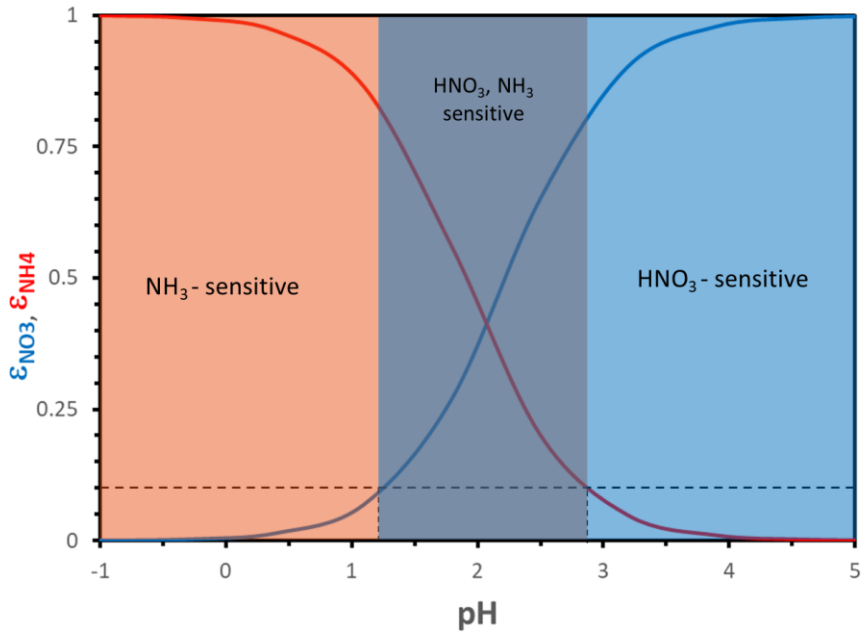
1
0.75
0.5
0.25
0
-1
0
1
2
3
4
5
pH
ε_{NO3}, ε_{NH4}
HNO_3, NH_3 sensitive
NH_3 - sensitive
HNO_3 - sensitive

(a)

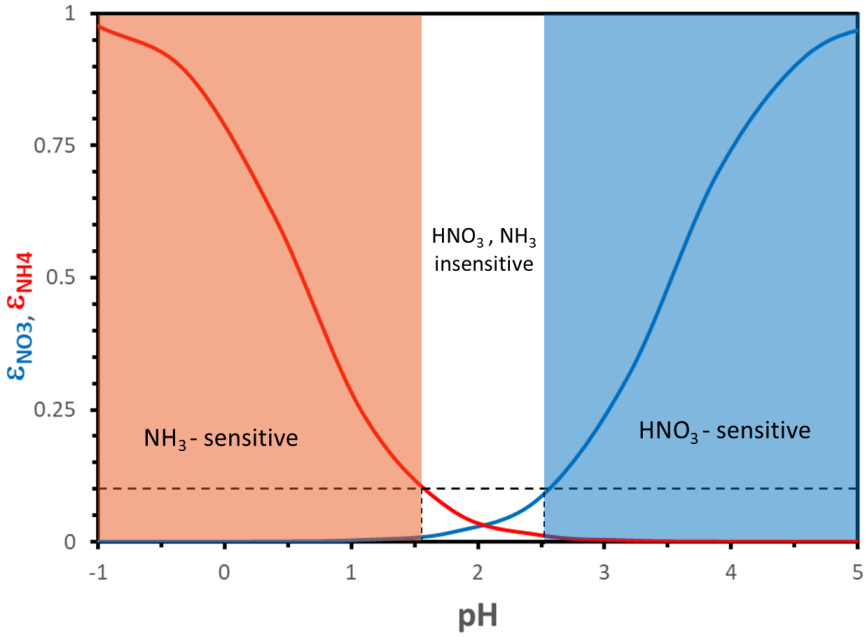
1
0.75
0.5
0.25
0
-1
0
1
2
3
4
5
pH
ε_{NO3}, ε_{NH4}
HNO_3 , NH_3 insensitive
NH_3 - sensitive
HNO_3 - sensitive

(b)

Figure 1.

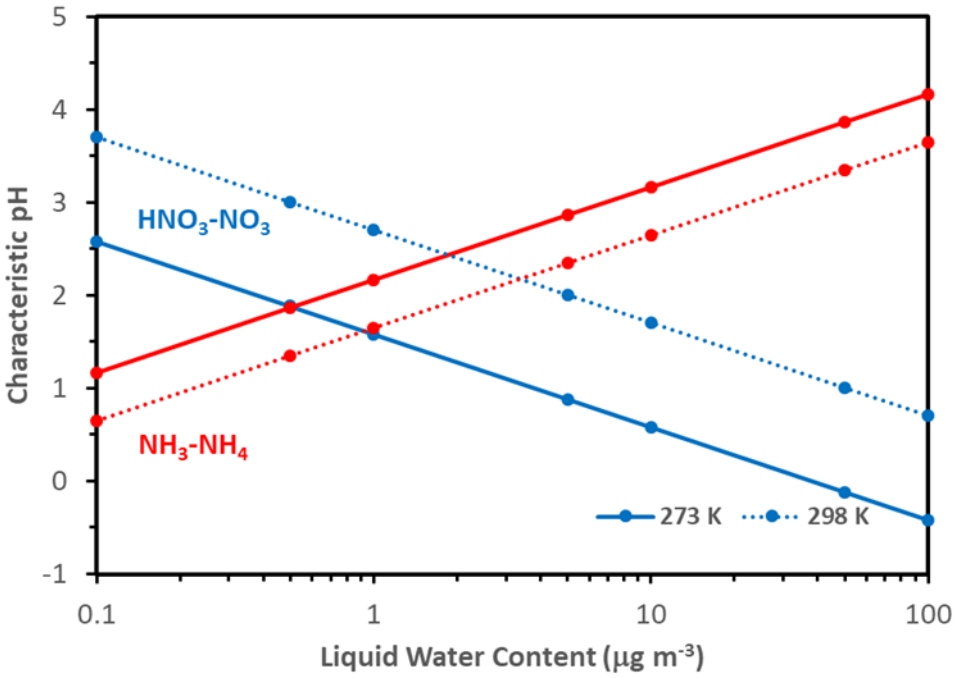
Characteristic pH
5
4
3
2
1
0
-1
0.1
1
10
100
Liquid Water Content (µg m-3)
HNO3-NO3
NH3-NH4
273 K
298 K

Figure 2.

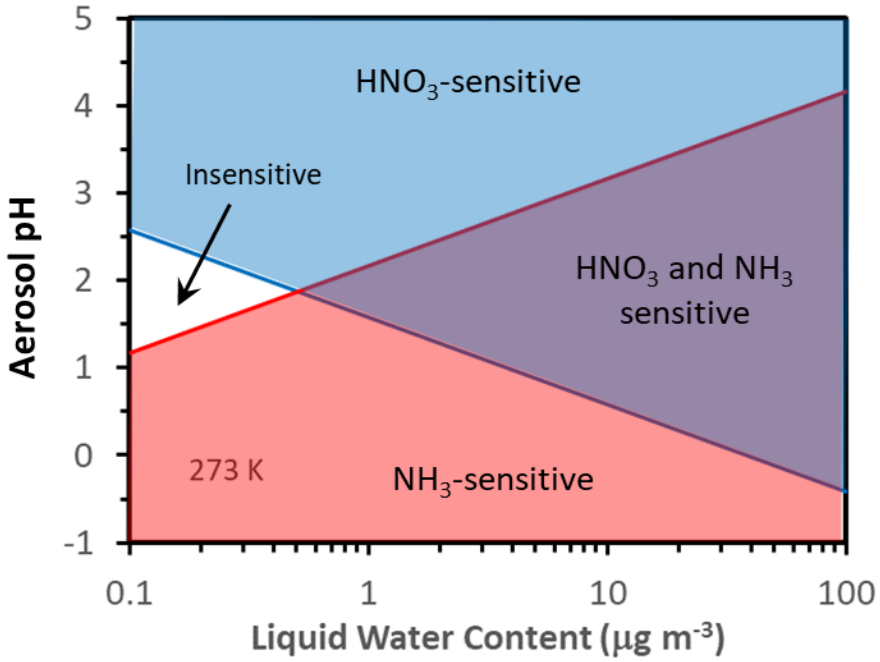
5
4
3
2
1
0
-1
Aerosol pH
HNO3-sensitive
Insensitive
HNO3 and NH3
sensitive
273 K
NH3-sensitive
0.1
1
10
100
Liquid Water Content (μg m-3)

(a)

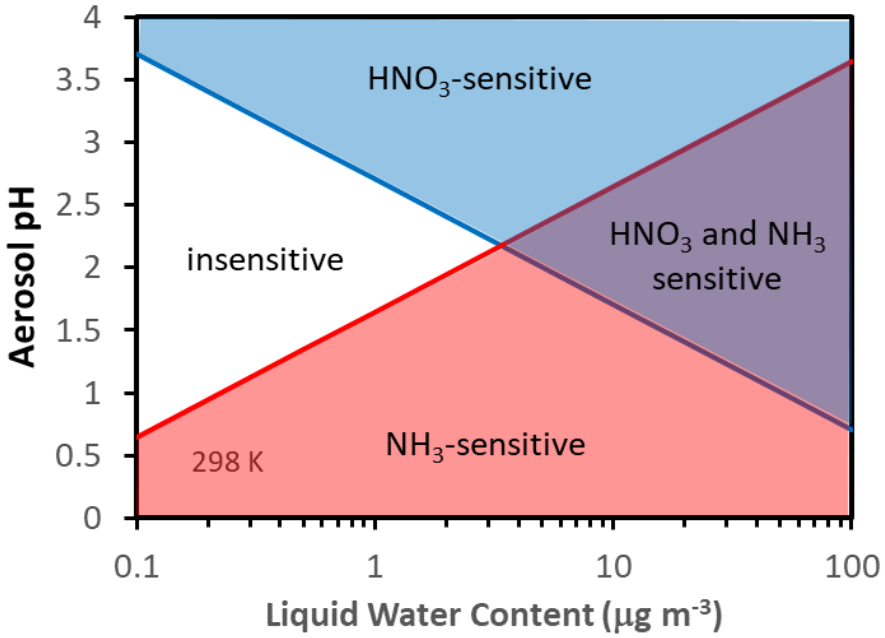
4
3.5
3
2.5
2
1.5
1
0.5
0
Aerosol pH
HNO3-sensitive
insensitive
HNO3 and NH3
sensitive
298 K
NH3-sensitive
0.1
1
10
100
Liquid Water Content (μg m-3)

(b)

Figure 3.

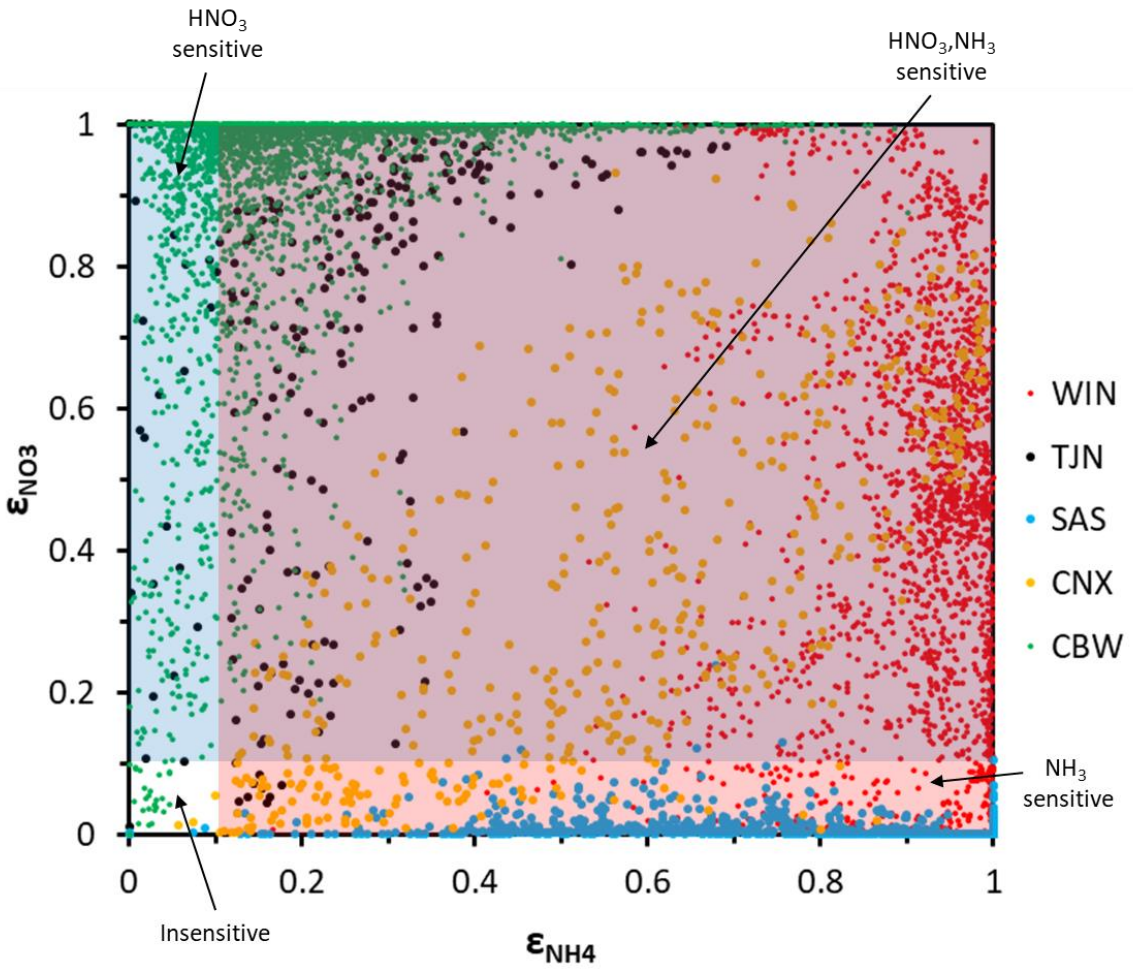
HNO3 sensitive
HNO3,NH3 sensitive
NH3 sensitive
Insensitive
WIN
TJN
SAS
CNX
CBW
εNO3
εNH4
0
0.2
0.4
0.6
0.8
1

Figure 4.

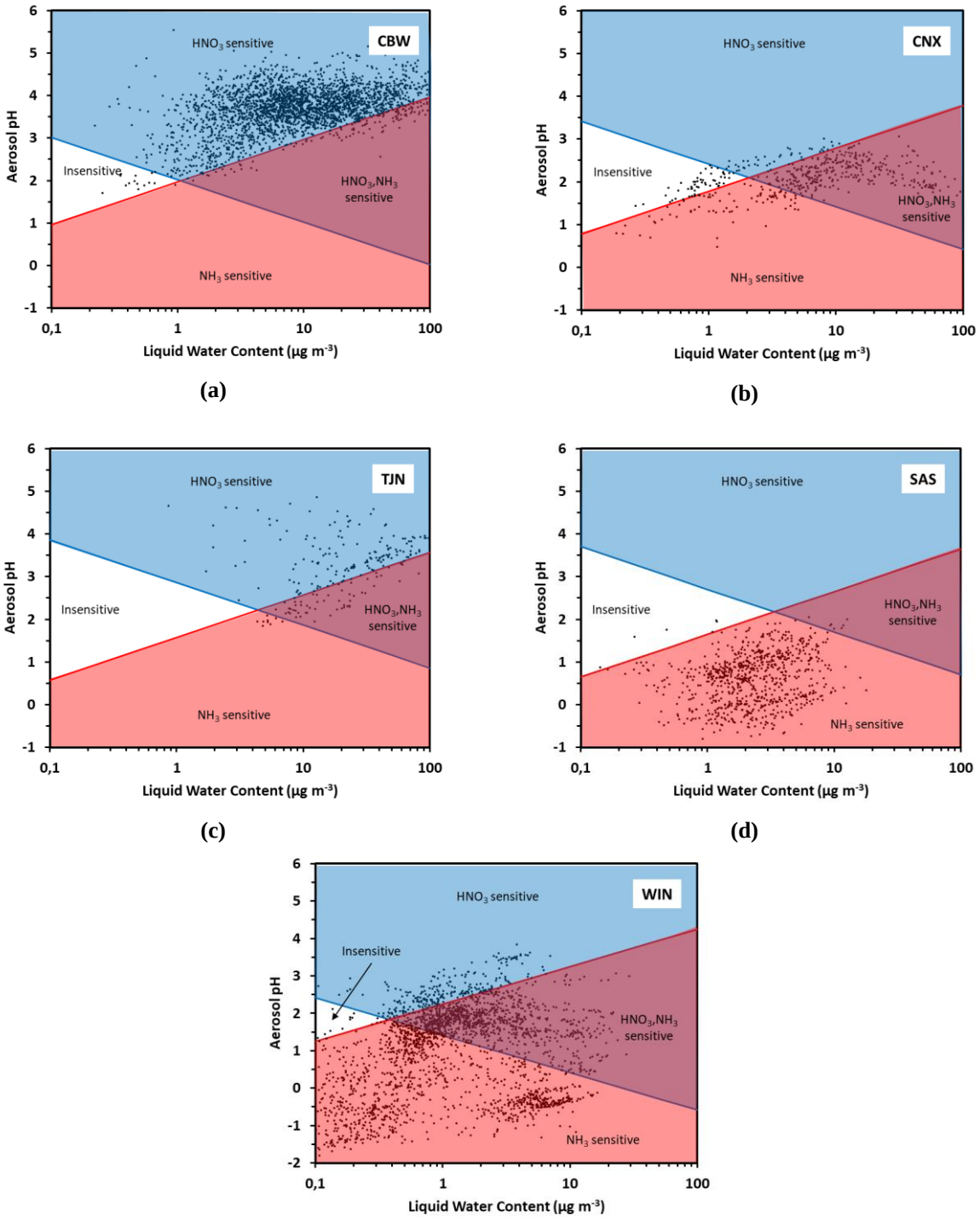
CBW
HNO3 sensitive
Insensitive
HNO3,NH3 sensitive
NH3 sensitive
Aerosol pH
Liquid Water Content (μg m-3)
(a)
CNX
(b)
TJN
(c)
SAS
(d)
WIN
(e)

Figure 5.